# Stereoselective Nitrile Hydrolysis by Immobilized Whole-Cell Biocatalyst

Praveen Kaul, Anirban Banerjee, and Uttam Chand Banerjee*

*Department of Pharmaceutical Technology, National Institute of Pharmaceutical Education and Research, Sector-67, SAS Nagar, Punjab, 160 062 India*

*Received October 21, 2005; Revised Manuscript Received February 23, 2006*

The present work attempts to deal with the stability and reusability aspect of nitrilase from *Alcaligenes faecalis* for the production of (*R*)-(−)-mandelic acid. Four entrapment matrixes were screened to search for a suitable support, and alginate was found to have significant process advantages over its other counterparts. Thermodynamic analysis allowed us to account for decreased enantioselectivity (*E*) as a result of immobilization. The system was also characterized based on the Thiele modulus ($\phi$). Efficient reusability of the biocatalyst up to 35 batches was achieved by immobilization as compared to 9 batches for free cells, and cross-linking extended it further to 40 batches. Finally, synthetic utility of the immobilized biocatalyst was demonstrated on a preparative scale to produce 640 g of (*R*)-(−)-mandelic acid with 97% enantiomeric excess (ee).

## Introduction

There is a considerable industrial interest in the enzymatic conversion of nitriles to their corresponding high-value carboxylic acids and amides.[1,2] Inspite of the great synthetic potential of nitrilases, their utilization as a versatile biocatalyst is largely unexploited. The lack of purified enzyme preparation has prompted the use of whole cell biocatalysts. Although commercial nitrilase preparations are available, they are too expensive for synthetic application. Immobilization of whole cells harboring the "expensive" nitrilase offers an "inexpensive" alternative to improve its reusability and stability. We have attempted to develop and characterize the most suitable matrix for entrapment of whole cells of *Alcaligenes faecalis* for the production of (*R*)-(−)-mandelic acid, a versatile chiral building block. *A. faecalis* has earlier been shown to harbor a nitrilase highly specific for arylacetonitriles.[3] (*R*)-(−)-Mandelic acid is a key intermediate for the production of semisynthetic cephalosporins[4] and penicillins.[5] It is also used as a chiral resolving agent[6] and chiral synthon for the production of antitumor agents[7] and anti-obesity agents.[8]

## Materials and Methods

**Chemicals.** Mandelonitrile, *n*-butyronitrile, sodium alginate, agarose, polyacrylamide, $\kappa$-carrageenan, glutaraldehyde (GA), and polyethyleneimine (PEI) were obtained from Sigma-Aldrich Chemical Co. (Milawukee, USA). Media components were obtained from Hi-Media Inc. (Mumbai, India). Inorganic salts, buffer salts, solvents and other chemicals were of highest purity and were obtained from standard companies.

**Microorganism and Cultivation Conditions.** The microorganism, *Alcaligenes faecalis* MTCC 126 was procured from Microbial Type Culture Collection (Institute of Microbial Technology, Chandigarh, India) and was grown in a medium of the following composition (g/L): ammonium acetate 10, peptone 5, yeast extract 5, dipotassium hydrogen phosphate 5, magnesium sulfate 0.2, ferrous sulfate 0.03, sodium chloride 1, and *n*-butyronitrile 3 (pH 7.2) in a 500 mL shake flask at 30 °C. After growth for 18 h, 3% (v/v) inoculum was transferred to fresh medium for enzyme production. Cells were harvested after 20 h by centrifugation at 12000*g* (4 °C) and washed with tris buffer (100 mM, pH 7.5) before use.

**Immobilization of Whole Cells.** For entrapment in alginate, cells were resuspended in the same buffer and added to sodium alginate solution (3%, w/v) and thoroughly mixed. The mixture was then added dropwise from a syringe to a stirred solution of calcium chloride (2%, w/v). After stirring for 2 h, beads were filtered through muslin cloth and stored in fresh calcium chloride solution of same composition until use. In the case of agarose, the harvested cells were washed, resuspended in tris buffer (100 mM, pH 7.5), mixed with 3% (w/v) agarose above gelling temperature, and allowed to cool. The resulting gel was cut in cubes (approximately 1 cm × 1 cm × 0.2 cm) and used as biocatalyst. For entrapment in $\kappa$-carrageenan, harvested cells were washed, resuspended in tris buffer (100 mM, pH 7.5), mixed with 3% $\kappa$-carrageenan (w/v) above gelling temperature, and allowed to cool. The resulting gel was cut in cubes (approximately 1 cm × 1 cm × 0.2 cm) and used as biocatalyst. Cells were entrapped in polyacrylamide by suspending them in tris buffer (100 mM, pH 7.5) containing 12% (w/v) acrylamide and 0.2% (w/v) bis-acrylamide. Subsequently ammonium persulfate (1.8%, w/v) and TEMED were added to produce polymerization. The resulting gel was cut in cubes (approximately 1 cm × 1 cm × 0.2 cm).

**Chemical Cross-Linking of Alginate Beads.** For chemical cross-linking, the immobilized biocatalyst was treated with GA and a mixture of GA and PEI. The immobilized catalyst was suspended in water containing 1.2 g of GA (50%) in 50 mL of water and stirred for 30 min at 20 °C. For cross-linking with GA and PEI, immobilized biocatalyst was treated with a solution of 3 g of PEI (25%) in 50 mL of water for 1 h under stirring at 20 °C and later treated with GA as explained. After cross-linking, the beads were washed thrice with water and stored in calcium chloride solution (2%, w/v) at 4 °C until further use.

**Biotransformation Conditions.** In the case of free cells, the standard reaction mixture (10 mL) consisted of wet cell paste (250 mg) suspended in tris buffer (100 mM, pH 7.5). Mandelonitrile (30 mM) was added to initiate the reaction and the mixture was incubated in a rotary shaker (30 °C, 200 rpm) for 6 h. Similar conditions were maintained for immobilized cells. The product was isolated and analyzed as explained previously.[9]

**Scanning Electron Microscopy (SEM).** The various immobilized preparations were dehydrated on a lyophilizer (Heto Dry Winer, Model

* Corresponding author. Telephone: 91-172-2214682-87. Fax: 91-172-2214692. E-mail: ucbanerjee@niper.ac.in.

10.1021/bm0507913 CCC: $33.50 
Published on Web 03/28/2006

**Table 1.** Screening of Entrapment Matrices Based on Efficiency, Effectiveness, and Recycling[a]

| matrix | cells retained after washing (mg) | immobilization efficiency (%) | activity after immobilization (U $mg^{-1}$ $min^{-1}$) | effectiveness parameter ($\eta$) | residual activity after 5 recycle (%) | cells leached out after 5 recycle (mg) |
|---|---|---|---|---|---|---|
| agarose | 186.78 | 93.39 | 6.87 | 0.687 | 86 | 36 |
| alginate | 200 | 100 | 5.51 | 0.551 | 100 | 0 |
| $\kappa$-carrageenan | 188.14 | 94.07 | 6.71 | 0.671 | 82 | 30 |
| polyacrylamide | 200 | 100 | 5.78 | 0.578 | 98 | 1.8 |

[a] Equal amounts of cells (250 mg) harboring 10 $Umg^{-1}$ $min^{-1}$ nitrilase activity were used for entrapment on each matrix. Each value represents an average of three readings. One unit of enzyme activity is defined as the amount of biocatalyst required to form 1 $\mu$M of acid under standard assay conditions.

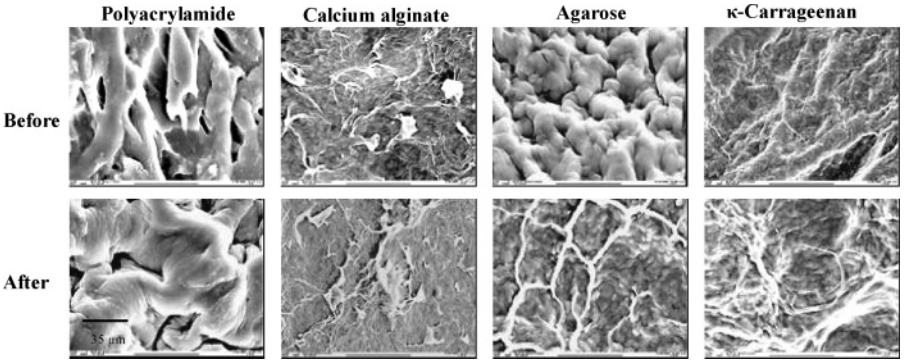


**Figure 1.** SEM pictures of various entrapment matrixes before and after 5 recycles.

DW-1-110, Denmark) and mounted on aluminum SEM stubs using a double sticky tape. The mounted samples were sputter coated with a thin layer of gold at 10 Torr vacuum (JEOL fine coat, Ion sputter, JFC 1100, Japan) and examined by electron microscopy (JEOL Electron Microscope, JSM 1600, Japan) at an acceleration potential of 1.2 kV.

## Results and Discussion

**Screening for Immobilization Matrix.** To improve the applicability of whole cell biocatalyst, various entrapment matrixes were screened based on their effect on initial reaction rate, conversion, selectivity, and also stabilization of the biocatalyst to allow its efficient reuse. Alginate and polyacrylamide entrapped cells showed highest immobilization efficiency, whereas carrageenan and agarose resulted in the least efficiency (Table 1). On the other hand, effectiveness ($\eta$) of immobilization showed a completely reverse trend. It was highest for agarose and carrageenan, whereas it was least for alginate and polyacrylamide. Effectiveness factor may be regarded as a measure of the mass-transfer limitations imposed by the matrix on the biocatalyst. It is defined as the ratio of actual reaction rate to that without diffusion (free biocatalyst). Reusability of the immobilized biocatalyst was also studied over a period of five batch reactions. It is evident that cell retention was least in agarose and this resulted in a severe drop in conversion over successive recycling. However, alginate and polyacrylamide entrapped cells showed the best reusability and conversion. Cell leaching was observed by optical microscopy by counting the cells in a hemocytometer. The surface erosion of matrixes after five recycles was visualized by SEM (Figure 1). Very little or no leaching (verified by optical microscopy) was observed in the case of polyacrylamide and alginate, which was also confirmed by their negligible surface erosion (verified by SEM). On the other hand, substantial surface erosion in the case of agarose and carrageenan confirmed cell leaching. The higher initial rates observed in agarose and carrageenan might also be explained by the higher cell leaching observed from these matrixes. Since a greater amount of free cells are available in the reaction mixture due to more leaching, the mass transfer limitations imposed by the matrix no longer exist and the reaction rate picks up. Another important characteristic of an immobilized biocatalyst is its stability. Thermostability is generally regarded as an overall index of stability of the biocatalyst, and hence, experiments were carried out to know thermal deactivation profiles of the immobilized biocatalyst (Figure 2). Thermal stability studies were carried out at 55 °C and residual activity was estimated at regular intervals. Protein deactivation has been proposed to follow a series-type pathway, involving different structural intermediates which may or may not retain activity comparable to the native form.[10] For the specific case of nitrilase from *A. faecalis*, the stable enzyme during its early stage of inactivation process is converted into a more labile but still active intermediate form. This inactivation is schematized in eq 1, where $(\text{nitrilase})_{\text{native}}$ is the native active form, $(\text{nitrilase})_{\text{labile}}$ is the labile intermediate, and $(\text{nitrilase})_{\text{d}}$ is the deactivated form.

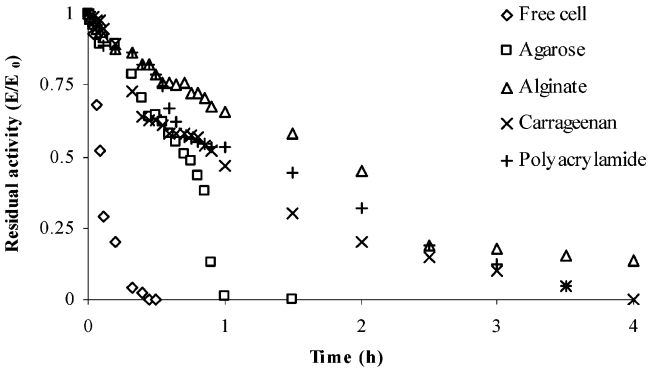


**Figure 2.** Thermal inactivation profiles of various whole-cell biocatalyst formulations.

$$(\text{nitrilase})_{\text{native}} \xrightarrow{k_{\text{i}}} (\text{nitrilase})_{\text{labile}} \xrightarrow{k_{\text{d}}} (\text{nitrilase})_{\text{d}} \qquad (1)$$

The −SH groups present in the nitrilase are often known to play a critical role in its deactivation.[11] Assuming that at time

**Table 2.** (a) First Order Inactivation Rate Constant ($k_d$), Correlation Coefficient ($r$), and Half Life ($t_{1/2}$) of Various Forms of Whole Cell Biocatalyst and (b) Model Parameters, Correlation Coefficient ($r$), and Half Life ($t_{1/2}$) for Series-Type Deactivation Study of Various Forms of Whole Cell Biocatalyst

(a)

| biocatalyst form | $k_d$ ($h^{-1}$) | $r$ | $t_{1/2}$ (h) |
|---|---|---|---|
| free cells | 9.80 | 0.982 | 0.07 |
| agarose | 1.34 | 0.974 | 0.51 |
| alginate | 0.54 | 0.965 | 1.27 |
| $\kappa$-carrageenan | 0.80 | 0.981 | 0.86 |
| polyacrylamide | 0.74 | 0.960 | 0.92 |

(b)

| biocatalyst form | $\alpha_i$ | $\alpha_d$ | $k_i$ ($h^{-1}$) | $k_d$ ($h^{-1}$) | $r$ | $t_{1/2}$ (h) |
|---|---|---|---|---|---|---|
| free cells | 0.62 | 0.0 | 1.07 | 3.89 | 0.987 | 0.15 |
| agarose | 0.68 | 0.0 | 0.09 | 3.50 | 0.977 | 0.74 |
| alginate | 0.81 | 0.04 | 0.73 | 2.10 | 0.988 | 1.42 |
| $\kappa$-carrageenan | 0.72 | 0.0 | 0.92 | 2.82 | 0.991 | 0.99 |
| polyacrylamide | 0.78 | 0.02 | 0.95 | 2.42 | 0.984 | 1.10 |

zero only the native enzyme is present, the total activity $a$ may be expressed by eq 2, where $k_i$ and $k_d$ are first-order rate constants and $\alpha_i$ and $\alpha_d$ are relative activity of the species $(\text{nitrilase})_{\text{labile}}$ and $(\text{nitrilase})_d$, respectively

$$a = \alpha_d + \left[1 + \frac{\alpha_i k_i}{k_d - k_i} - \frac{\alpha_d k}{k'_d - k_i}\right] \exp(-k_i t) - \left[\frac{\alpha_i k_i}{k_d - k_i} - \frac{\alpha_d k_i}{k_d - k_i}\right] \exp(-k_d t) \quad (2)$$

As expected, for $\alpha_i = 0$, the eq 2 yields the classical first-order deactivation rate expression: $a = \exp(-k_i t)$. The deactivation profile was fitted using both two-step and first-order deactivation model (Table 2, parts a and b). As the results indicate, the two-step model resulted in better fitting than the latter and afforded accurate estimation of half-life ($t_{1/2}$). It may be inferred that alginate resulted in significant stabilization of the whole cell biocatalyst compared to other matrixes. From the results discussed so far, it is clear that alginate entrapped whole cells offer significant process advantages over other entrapment matrixes, and therefore, it was chosen for further studies.

**Effect of Temperature and pH.** The effect of temperature on the initial reaction rate, conversion, and optical purity was studied in the range of 20−65 °C. It was observed that the initial reaction rate was highest at 50 °C for free cells, and it shifted to 55 °C for immobilized cells. The immobilized cells also exhibited a greater reaction rate than free cells at 65 °C indicating greater stabilization of the system (Figure 3a). However, conversion was maximum at 37 °C for both free and immobilized cells (Figure 3b), which indicates a very complex effect of temperature and assay duration on the true temperature optima of nitrilase. Activation energy to form the enzyme substrate complex was found to drop from 6.89 to 6.18 kcal/mol due to immobilization (inset Figure 3a) thus indicating improvement in the property of biocatalyst, as it required less energy to form the transition state. As the temperature was increased, there was a slight decrease in enzyme enantioselectivity. Moreover, lowering the temperature has also been shown to be a useful technique to enhance enantioselectivity of the enzyme.[12] The enantiomeric ratio ($E$) in enzymatic kinetic

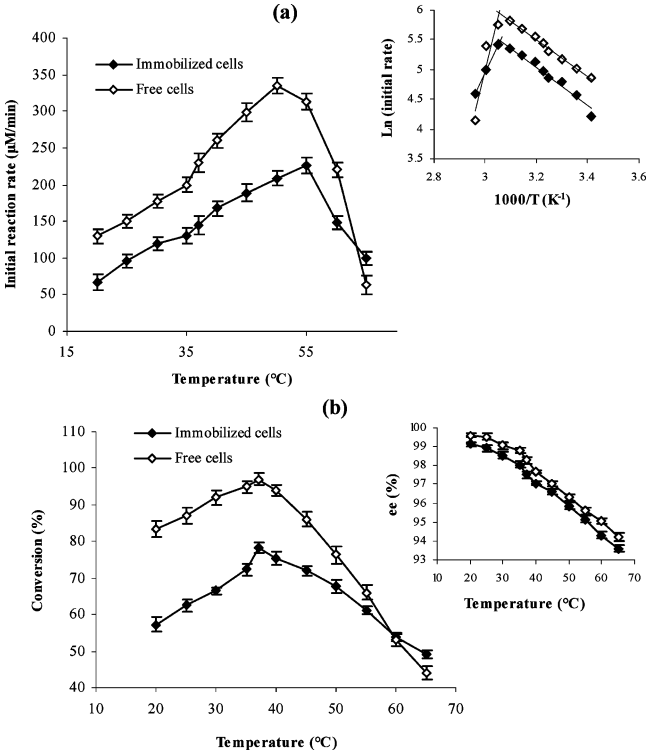


**Figure 3.** Effect of temperature on (a) initial reaction rate (Arrhenius plot in inset) and (b) conversion and ee (inset).

resolution is often temperature dependent. This is explained by eqs 3−5 where $\Delta\Delta H^{\ddagger}$ is the enthalpy of activation, $\Delta\Delta S^{\ddagger}$ is the free entropy of activation, and $\Delta\Delta G^{\ddagger}$ is the free energy of activation of paths of two enantiomers.

$$\Delta\Delta G^{\ddagger} = -RT \ln E \quad (3)$$

$$\Delta\Delta G^{\ddagger} = \Delta\Delta H^{\ddagger} - T\Delta\Delta S^{\ddagger} \quad (4)$$

Equating eq 3 and 4, we get

$$\ln E = \Delta\Delta S^{\ddagger}/R - \Delta\Delta H^{\ddagger}/(RT) \quad (5)$$

Another relevant parameter is the racemic temperature ($T_r$), at which there is no discrimination of the enantiomer ($T_r = \Delta\Delta H^{\ddagger}/\Delta\Delta S^{\ddagger}$). An attempt was made to study the effect of temperature on enantioselectivity ($E$), for both free and immobilized cells. For this purpose, conversion between 0 and 50% were taken. It was observed that lowering the temperature resulted in enhanced enantioselectivity (Figure 4); however, an inevitable problem was the decrease in reaction rate resulting in the increased turnover time. The study allowed separation of contributions from $\Delta\Delta H^{\ddagger}$ and $\Delta\Delta S^{\ddagger}$ to the interaction of the substrate with the binding pocket of nitrilase. The nitrilase from *A. faecalis* prefers the ($R$) enantiomer of this chiral substrate, and the enzyme substrate complexation is enthalpically favored ($\Delta\Delta H^{\ddagger}$ is negative) but entropically unfavored ($\Delta\Delta S^{\ddagger}$ is negative; Table 3). This implies that the entropic component counteracts the enthalpic component to yield a low selectivity. Additionally, immobilized cells showed a decrease in enantioselectivity as compared to the free cells. It is evident from eq 3, that a greater negative value of $\Delta\Delta G^{\ddagger}$ results in higher selectivity due to the higher free energy advantage of the fast reacting enantiomer. In the case of the free biocatalyst, the ($R$) enantiomer experiences very little competition from the ($S$) enantiomer due to its better steric fit in the active site, and hence, higher enantioselecivity is observed. However, when the biocatalyst was immobilized,

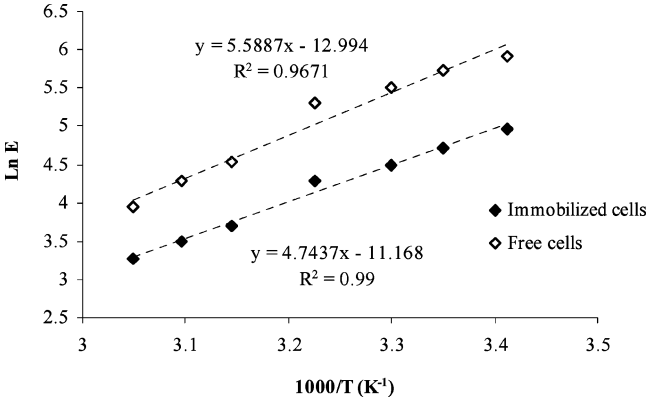


**Figure 4.** Correlation between ln $E$ vs $1/T$ for nitrile hydrolysis. $E = \ln[1 - c(1 + ee_p)]/\ln[1 - c(1 - ee_p)]$ where $c$ is conversion and $ee_p$ is enantiomeric excess of product.

**Table 3.** Differential Thermodynamic Parameters for Mandelonitrile Hydrolysis

| biocatalyst form | $\Delta\Delta H^{\ddagger}$ (kcal/mol) | $\Delta\Delta S^{\ddagger}$ (cal/mol) | $T_r$ (°C) |
|---|---|---|---|
| free cells | −11.10 | −25.81 | 157.06 |
| immobilized cells | −9.42 (15.13)[a] | −22.19 (14.02)[a] | 151.51 |

[a] Values in parentheses represent % change in $\Delta\Delta H^{\ddagger}$ and $\Delta\Delta S^{\ddagger}$ as a result of immobilization.

the matrix did not show any enantio preference for the substrate enantiomers which affects the local concentration of the enantiomers and leads to an altered state of reaction kinetics due to the diffusion restriction. This results in a change in kinetics of presentation of the enantiomers to the active site, and the fast reacting (*R*) enantiomer now experiences greater competition from the slow reacting (*S*) enantiomer for its interaction with the enzyme active site and loses its enthalpic edge thus, leading to a decrease in enantioselectivity (Figure 5). Immobilization resulted in a 14.02% change in $\Delta\Delta S^{\ddagger}$ (a higher negative value would decrease $\Delta\Delta G^{\ddagger}$) in favor of enantioselectivity and also a 15.13% change in $\Delta\Delta H^{\ddagger}$ to oppose the enantioselectivity (Table 3). It may be regarded that, in the clash between entropy and enthalpy, the latter had an upper hand, and as a result of concomitant variation in $\Delta\Delta H^{\ddagger}$, there is an overall decline in enantioselectivity (*E*) in case of the immobilized cells. This change in $\Delta\Delta H^{\ddagger}$ as a result of immobilization implies that the fast reacting (*R*) enantiomer is not able to interact effectively with the enzyme active site, and therefore, the enantioselectivity drops.

The pH of the reaction mixture had a significant effect not only on enzyme activity and conversion but also on the optical purity of (*R*)-(−)-mandelic acid. Under kinetic conditions, the unreacted (*S*) substrate enantiomer complicates its separation from the product of interest. However, by adjusting the pH to alkaline, the (*S*)-mandelonitrile can be funneled back into the racemization pathway (Scheme 1). This racemization via spontaneous dissociation was also found to be dependent on pH and was accelerated under alkaline condition; however, the enzyme activity was found to be highest at pH 7.5. The optical purity of the product increased with the increase of pH from acidic to slightly alkaline; however, the conversion was maximum at pH 8, thus confirming the synergic effect of racemization on enantioselectivity (Figure 6, panels a and b).

**Effect of Cell Loading and Bead Diameter on Effectiveness of Immobilization.** Effectiveness of the immobilized system increased with the increase of cell loading. Beads with a cellular concentration of 2.5 mg cell/mg alginate displayed highest $\eta$;

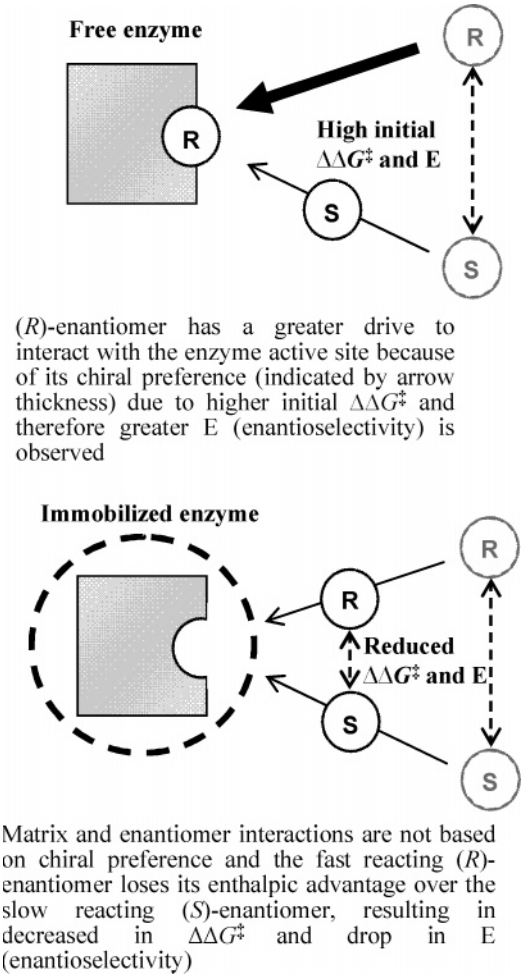


**Figure 5.** Schematic explanation for decreased enantioselectivity (*E*) due to immobilization.

however, beyond this value there was a drop in enzyme activity. This behavior shows that kinetic conditions prevail at cell loading up to 2.5 mg cell/mg alginate, and at higher cell loading, diffusion restriction to the substrate becomes the rate controlling step (Figure 7).

Effect of different bead sizes on $\eta$ was also elucidated (Table 4). At lower bead diameter, $\eta$ approached that of the free cell ($\eta = 1$). Larger beads had a smaller $\eta$, implying that there was more diffusion limitation which is also indicated by the values of the diffusion coefficient ($D_e$). The value of $\eta$ is a measure of mass transfer effect. For $\eta < 1$, the process is diffusion limited. $\eta$ approaches 1 for small values of $\phi$ and the intraparticle diffusion has no effect on the enzymatic reaction. On the other hand, the intraparticle diffusion has a large effect on the reaction for $\phi > 5$ (see footnote in Table 4).[13]

**Chemical Cross-Linking and Recycling of Alginate Beads.** To improve the operational stability and reusability of the immobilized system, chemical cross-linking of alginate beads was attempted using GA and a combination of PEI and GA. The effect of cross-linking on enzyme stabilization was studied by incubating the biocatalyst formulations at 60 °C for a period of 1.5 h and estimating residual activity. It was found that cross-linking resulted in greater stabilization of the biocatalyst at the cost of further escalation of the mass transfer problem (Table 5). Analysis of variance revealed that there was no statistically significant difference between residual activities of the beads cross-linked with GA alone or GA + PEI ($p < 0.05$). Alginate beads cross-linked with GA caused greater mass transfer

**Scheme 1.** Scheme for Dynamic Resolution of Mandelonitrile by Nitrilase

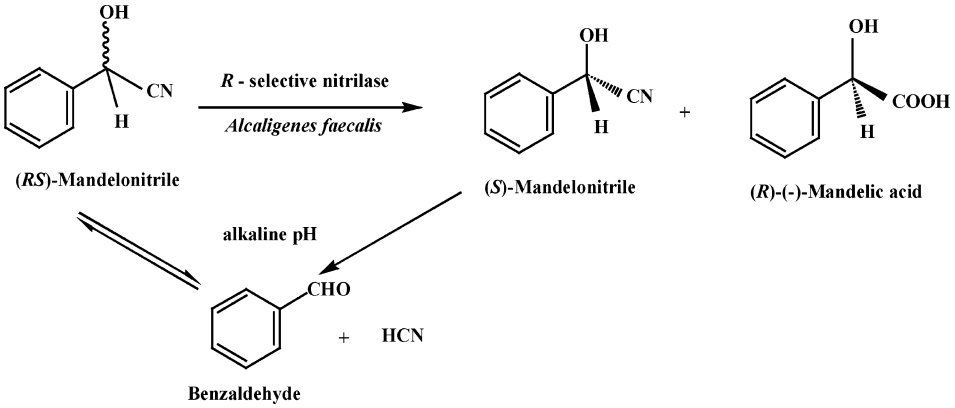


**Table 4.** Effect of Bead Diameter ($d_p$) on Reaction Rate and Effectiveness Factor

| $d_p$ (cm) | $v$ (mg g$^{-1}$ h$^{-1}$) | $\eta$ | $\phi^a$ | $K' \times 10^{-3}$ (cm$^3$ cm$^{-3}$ s$^{-1}$)$^b$ | $D_e \times 10^{-6}$ (cm$^2$ s$^{-1}$)$^c$ |
|---|---|---|---|---|---|
| free cells | 26.01 | 1 | | | |
| 0.18 | 17.09 | 0.65 | 3.1 | 0.9138 | 3.63 |
| 0.24 | 14.37 | 0.55 | 4.3 | 0.7684 | 2.82 |
| 0.32 | 11.44 | 0.44 | 5.6 | 0.6121 | 2.35 |
| 0.38 | 10.29 | 0.39 | 6.4 | 0.5501 | 2.28 |

[a] $\eta = 3/\phi\,[(1/\tanh\phi) - (1/\phi)]$. [b] $K' = k \times \rho_P$ (where $K'$ is the rate constant, $k$ is the first-order reaction rate constant, and $\rho_P$ is the density of the dried cell). [c] $\phi = R\sqrt{(K'/D_e)}$ (where $D_e$ is the effective diffusivity of nitrile within the bead and $R$ is the bead radius).

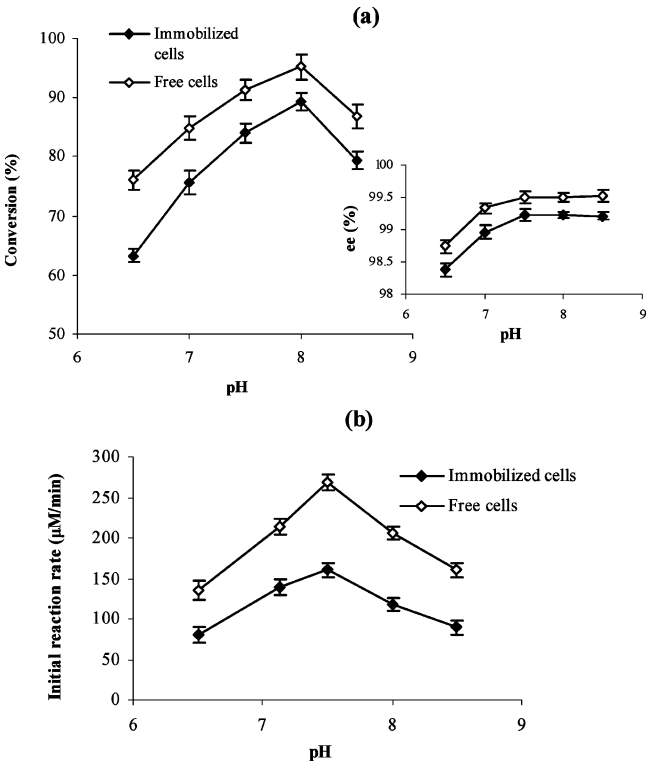


**Figure 6.** Effect of pH on (a) initial reaction rate and (b) conversion and ee (inset).

**Table 5.** Effect of Cross Linking on Stability and Effectiveness Factor

| biocatalyst form | residual activity after heat treatment at 60 °C (%) | effectiveness factor ($\eta$) | time for completion of reaction |
|---|---|---|---|
| free cells | 0 | 1 | 5 |
| control | 15 | 0.67 | 8 |
| GA | 24 | 0.50 | 15 |
| GA+PEI | 25 | 0.57 | 12 |

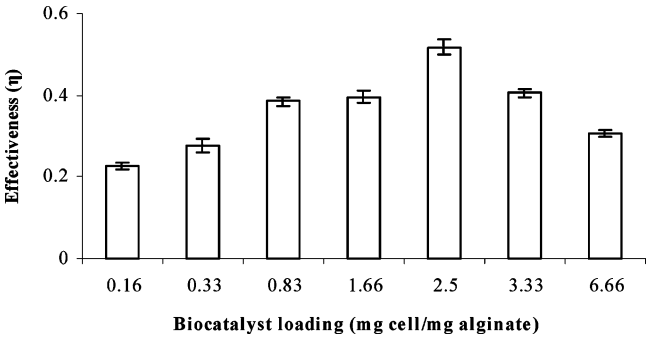


**Figure 7.** Effect of biocatalyst loading on effectiveness factor.

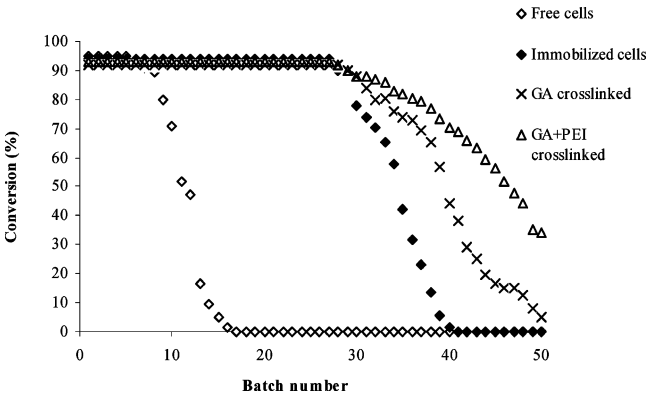


**Figure 8.** Reuse of free and alginate immobilized whole cells.

restriction than beads cross-linked with GA + PEI and, therefore, required more time to drive the reaction to completion. Reusability of various biocatalyst formulations was assessed in batch mode, and it was found that immobilization resulted in efficient recycling of the biocatalyst retaining almost 100% activity till 30 consecutive batches as compared to 9 batches for free cells. A further increase in recycle efficiency was achieved up to 40 batch reactions by cross-linking of alginate beads (Figure 8). GA + PEI was chosen as the method of choice over GA cross-linking considering the effectiveness parameter ($\eta$).

**Preparative-Scale Reaction with Immobilized Biocatalyst.** The nitrile hydrolysis was scaled-up in a 100 mL stirred tank, jacketed reactor. *A. faecalis* was grown in a 2 l Bioflo 3000 bioreactor (New Brunswick Scientific, Edison, NJ). The fer-

mentation was carried out at 30 °C (150 rpm, 1 vvm) for 12 h. Harvested cells were immobilized and cross-linked as explained earlier. To the reaction mixture containing alginate beads in buffer, was added 39.64 g of mandelonitrile in every batch reaction. The system was run for 15 such consecutive batches to produce a total of 640 g of (*R*)-(−)-mandelic acid with an optical purity of 97% ee. The immobilized biocatalyst retained 100% activity and was stored in 2% calcium chloride solution at 4 °C until further use. The catalyst productivity for the entire series of reactions was 85.3 g of (*R*)-(−)-mandelic acid/g wet cell weight and the volumetric productivity of the initial reaction in the series was 35.5 g of product/L/h.

## Conclusion

Inspite of the recognition of the synthetic potential of nitrilases, their successful integration into industrial scale processes is far from being successfully executed. Any biocatalytic process demands a continuous supply of a reusable, stable, and active biocatalyst formulation with an overall low cost. Immobilization offers a means to stretch the shelf life of a biocatalyst; however, the support should be cheaply available and the immobilization protocol should be scalable and simple to adopt. An intensive screening was carried out for entrapment support matrixes for the immobilization of whole cells of *A. faecalis*, and alginate immobilized cells were found to offer sizable improvement in the properties of the whole cell biocatalyst. After choosing the most suitable entrapment matrix, operational conditions for biotransformation were optimized. An inverse relation between the assay duration and temperature optima was found, and the study also allowed us to segregate the enthalpic and entropic contributions to the binding of the substrate to the enzyme active site. Effect of pH suggested that the substrate recycling via spontaneous degradation was more effective at alkaline pH (8.5); however, the enzyme functioned best at slightly alkaline pH (7.5). Analysis of mass transfer through the immobilized system indicated a greater diffusion resistance at higher biocatalyst loading and bead diameter. Additionally, the system was also characterized based on the Thiele modulus ($\phi$). Efficient biocatalyst recycling was achieved as a result of immobilization, and moreover, chemical cross-linking with GA + PEI allowed its operational life to be further extended. Finally, alginate-immobilized cells were utilized on a preparative scale for 15 consecutive batches to produce 640 g of optically pure (*R*)-(−)-mandelic acid (97% ee).

**Acknowledgment.** P.K. and A.B. gratefully acknowledge the fellowship provided by CSIR, Government of India. This is NIPER communication number 369.

## References and Notes

(1) Banerjee, A.; Sharma, R.; Banerjee, U. C. *Appl. Microbiol. Biotechnol.* **2002**, *60*, 33−44.
(2) Kobayashi, M.; Shimizu, S. *Curr. Opin. Chem. Biol.* **2000**, *4*, 95−102.
(3) Yamamoto, K.; Oishi, K.; Fujimatsu, I.; Komatsu, K. I. *Appl. Environ. Microbiol.* **1991**, *57*, 3028−3032.
(4) Terreni, M.; Pagani, G.; Ubiali, D.; Fernandez −Lafuente, R.; Mateo, C.; Guisan, J. M. *Bioorg. Med. Chem. Lett.* **2001**, *11*, 2429−2432.
(5) Furlenmeier, A.; Quitt, P.; Vogler, K.; Lanz, P. U.S. Patent No. 3,957,758, 1976.
(6) Kinbara, K.; Sakai, K.; Hashimoto, Y.; Nohira, H.; Saigo, K. *Tetrahedron: Asymmetry* **1996**, *7*, 1539−1542.
(7) Surivet, J. P.; Vatèle, J. M. *Tetrahedron* **1999**, *55*, 13011−13028.
(8) Mills, J.; Schmiegel, K. K.; Shaw, W. N. U.S. Patent No. 4,391,826, 1983.
(9) Banerjee, A.; Kaul, P.; Banerjee, U. C. *Arch. Microbiol.* **2006**, *184*, 407−418
(10) Henley, J. P.; Sadana, A. *Enzyme Microb. Technol.* **1985**, *7*, 50−60.
(11) Kobayashi, M.; Komeda, H.; Yanaka, N.; Nagasawa, T.; Yamada, H. *J. Biol. Chem.* **1992**, *267*, 20746−20751.
(12) Phillips, R. *Enzyme Microb. Technol.* **1992**, *14*, 417−419.
(13) Tanaka, H.; Matsumara, M.; Veliky, I. A. *Biotechnol. Bioeng.* **1984**, *26*, 53−58.

BM0507913